

Magnetic nanocables—Silicon carbide sheathed with iron-oxide-doped amorphous silica

C. Liu,^{a)} R. W. Li, A. Belik, D. Golberg, and Y. Bando

International Center for Young Scientists, National Institute for Materials Science, Namiki 1-1, Tsukuba, Ibaraki 305-0044, Japan

H. M. Cheng

Shenyang National Laboratory for Materials Science, Institute of Metal Research, Chinese Academy of Sciences, 72 Wenhua Road, Shenyang 110016, China

(Received 12 September 2005; accepted 1 January 2006; published online 24 January 2006)

High-purity nanocables of iron-containing amorphous-silica-sheathed silicon carbide were synthesized by a thermal reaction method using silicon wafer as the silicon source and growth substrate, and ferrocene as the carbon and iron catalyst precursor. The nanocables were tens of μm in length and 40–60 nm in diameter. Iron oxide nanoparticles with a mean diameter of 5 nm were dispersed evenly in the amorphous silica layer. The nanocables were found to be ferromagnetic at both 10 K and room temperature, which indicates that they may have important potential applications in electromagnetic nanodevices. © 2006 American Institute of Physics.

[DOI: 10.1063/1.2167787]

One-dimensional (1D) nanostructured materials attract extensive research interest due to their novel physical and chemical properties, and prospective applications. Among them, so-called nanocables—that contain metallic or semiconducting cores and coaxial insulating shells—have recently been studied intensively.^{1–25} These unique core-shell structures provide additional opportunities for enhancing the functionality of 1D nanostructures, and may find applications in nanoscale heterostructured electronic devices. On the other hand, nanostructured magnetic materials are considered to be promising building blocks of information storage and spintronic devices.²⁶ It is therefore foreseeable that magnetic nanocables may have potential applications in various multifunctional electromagnetic nanodevices.

Very recently, Crowley *et al.*²⁷ reported the magnetic properties of a coaxial heterostructure of germanium nanowire surrounded by cobalt nanotube sheath. However, to the best of our knowledge, there has been no report on magnetic nanocables that contain a conductive core and an insulating sheath layer so far. In this study, we report on the synthesis and magnetic properties of nanocables composed of silicon carbide core and iron oxide-implanted amorphous-silica sheath.

The synthesis was performed in a quartz tube reactor inserted into a horizontal tubular furnace. A (100) one-side polished silicon wafer with an approximate size of 10 mm \times 15 mm was ultrasonically cleaned in ethanol and then in deionized water. The cleaned silicon wafer was put onto a graphite plate and placed in the constant temperature region of the tubular furnace. A Fe_2O_3 powder was loaded in a ceramic boat, which was put upstream in the reactor. A ferrocene tablet with a diameter of 10 mm, cold pressed from a powder, was located near the edge of the tubular furnace (upstream of the Fe_2O_3 and Si wafer). High-purity (99.999%) hydrogen gas was used as a carrier gas at a con-

stant flux of 70 ml/min. The furnace temperature was increased to 1150 °C at a rate of 20 °C/min and kept for 30 min, then the power source was switched off and the furnace cooled down to the room temperature. A uniform layer of gray-white fluffy substance with a thickness of 1–2 mm was formed on the surface of the silicon wafer. The as-prepared samples were characterized using a field emission scanning electron microscope (SEM) and a high-resolution transmission electron microscope (HRTEM) equipped with a Ω -type energy filter and an x-ray energy dispersive spectrometer (EDS). The magnetic properties of the nanocables were studied by using a superconducting quantum interference device magnetometer. During the magnetization measurements, the nanocables were packed in a capsule randomly.

Figure 1 displays the typical SEM image of an as-synthesized product on a silicon wafer. Numerous entangled nanowires can be seen. The nanowires are of high purity; no catalyst particles and attached impurities can be observed. The nanowires have a mean diameter of ~ 50 nm and lengths

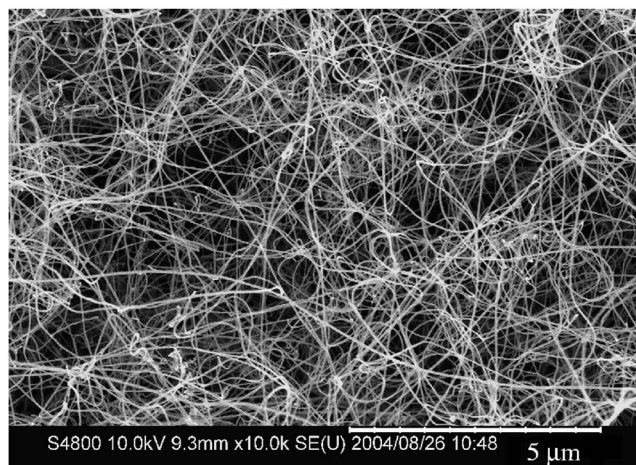


FIG. 1. SEM image of a product found on the silicon wafer, revealing clean entangled nanowires with a mean diameter of ~ 50 nm.

^{a)}Also at: Shenyang National Laboratory for Materials Sciences, Institute of Metal Research, Chinese Academy of Sciences, 72 Wenhua Rd., Shenyang 110016, China; electronic mail: cliu@imr.ac.cn

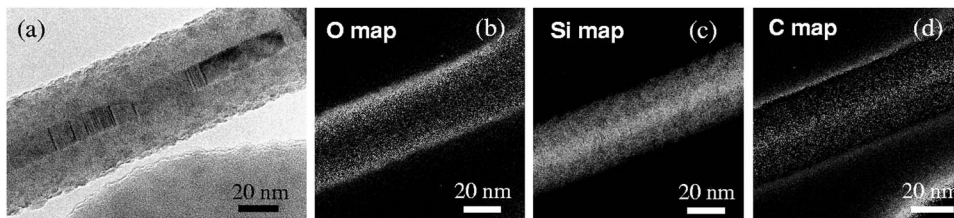


FIG. 2. TEM image (a) of a silicon oxide sheathed silicon carbide nanocable, and the corresponding spatially resolved oxygen (b), silicon (c), and carbon (d) elemental maps.

up to tens of micrometers. Many curled and bent structures are visible within the nanowires. As a rule, the nanowires are parallel to the surface of the silicon wafer substrate.

Transmission electron microscopy (TEM) observations revealed that the nanowires have a core-shell structure, as shown in Fig. 2(a). The corresponding oxygen, silicon, and carbon [Figs. 2(b)–2(d)] elemental maps documented that the central part of a nanostructure is composed of silicon and carbon, whereas on the periphery the silicon and oxygen signals are prevailing. HRTEM observations show that a sheath layer is made of an amorphous substance, whose thickness is typically in the range of 15–20 nm [Fig. 3(a)]; and the central part is crystalline, displaying the lattice fringes separated with a distance of ~ 0.25 nm [Fig. 3(b)]. Combining the results of elemental mapping and selected area electron diffraction pattern taken from the central part of the cable [see inset of Fig. 3(b)], we conclude that the core of the cable consists of a β -SiC single crystal growing along the $\langle 111 \rangle$ direction. The diameter of the SiC core is usually ~ 10 nm. EDS spectrum recorded from the sheath layer displays sharp peaks of silicon and oxygen, coinciding well with the results of elemental mapping, and the atomic ratio of oxygen to silicon is

slightly above 2:1. It is therefore indicated that the sheath layer is made of amorphous silica.

As opposed to the pure silicon oxide nanowires or silicon oxide shell layers within nanocables reported by other researchers,^{1–4} we observed a dark contrast particles with diameters in the range of 3–10 nm dispersed evenly in the silicon oxide sheath layers [see Figs. 2(a) and 3(a)]. Since a small amount of iron can be detected by EDS analysis, the particles are thought to consist of an iron compound.

Figure 4 shows the magnetization versus magnetic field curves of the nanocables measured at 10 K and room temperature. We observe hysteresis loops clearly at both low temperature [Fig. 4(a)] and room temperature [Fig. 4(b)]. This implies that the nanocables are ferromagnetic. The coercive field (H_c) of the nanocables was measured to be 350 Oe and 100 Oe at 10 K and 300 K, respectively. Since the constituting silicon carbide and silicon oxide are diamagnetic or weakly paramagnetic (in the case of defect presence), the ferromagnetic feature of the nanocables is concluded to be due to iron-containing nanoparticles dispersed in the amorphous-silica layer. Considering that the atomic

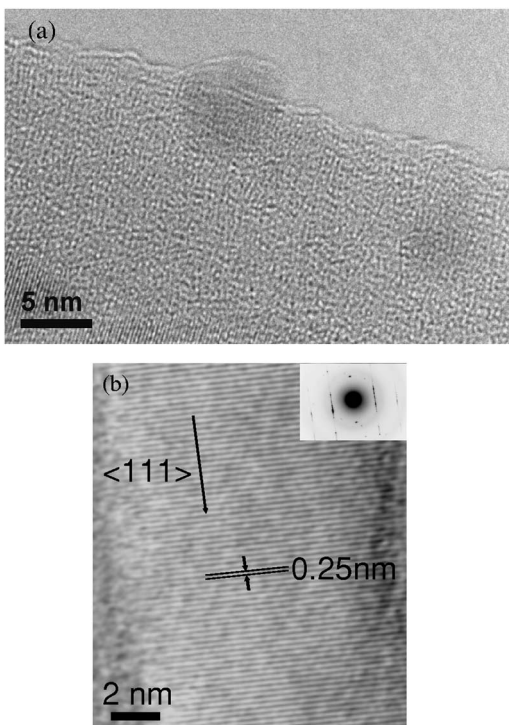


FIG. 3. HRTEM images of an amorphous-silicon oxide sheath (a) and a crystalline silicon carbide core (b). The silicon oxide layer is typically 15–20 nm thick, and its boundary with the silicon carbide core is wavy. Iron oxide nanoparticles with diameter of ~ 5 nm can be seen dispersed in the silicon oxide layer. The silicon carbide core is ~ 10 nm in diameter. It grows along the $\langle 111 \rangle$ direction, displaying an interplanar distance of 0.25 nm. Inset is the corresponding electron diffraction pattern.

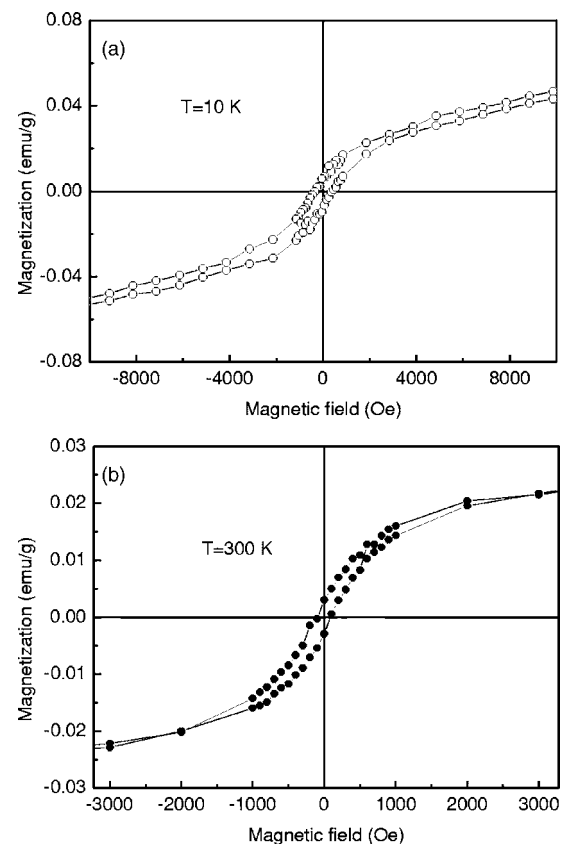
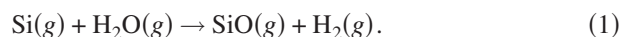


FIG. 4. Normalized magnetization (M)-magnetic field (H) curves of the nanocables measured at 10 K (a) and room temperature (b). The diamagnetic and possible weakly paramagnetic background caused by the capsule, silicon carbide core, and silicon oxide sheath have been subtracted.

ratio of oxygen to silicon is slightly higher than 2:1, and that Fe_3O_4 and $\gamma\text{-Fe}_2\text{O}_3$ are ferromagnetic with the Curie temperatures of 850 K and 958 K, respectively, it is therefore reasonable to assume that the nanoparticles contain mainly iron oxide (Fe_3O_4 or $\gamma\text{-Fe}_2\text{O}_3$).

The present nanocables were synthesized by a simple one-step thermal reaction, and the growth process is suggested to be as follows. When the furnace temperature was increased to a certain value, ferrocene put at the upper stream would be vaporized and carried into the high-temperature region of the reactor by a hydrogen gas flow. Then, the ferrocene decomposed into iron and carbon or hydrocarbons. Some iron clusters may aggregate onto the surface of a silicon wafer. Due to small dimensions, Si-Fe binary phase or Si-Fe-O ternary phase liquid drops might form on the silicon wafer, even though the furnace temperature (1150 °C) is lower than the corresponding eutectic temperatures. With the increase in silicon concentration within the liquid droplets, a silicon vapor appeared in the vicinity of the silicon wafer. The vaporized silicon would be oxidized into SiO by a H_2O vapor (from the reducing of the Fe_2O_3 powder by H_2) in line with the equation:



Carbon atoms resulted from the decomposition of ferrocene then reacted with SiO in accord with the equation:



Once formed, SiC grew preferentially along the $\langle 111 \rangle$ direction; whereas an amorphous-silicon oxide formed an outer shell.² Thus, the silicon oxide-sheathed SiC nanocables were resultantly formed. During the nanocable growth, iron clusters from the continuous decomposition of ferrocene were oxidized into iron oxides by a water vapor. Carried by the gas flow, the iron oxide clusters collided with the silicon oxide layers, and finally formed embedded nanoparticles dispersed evenly in a sheath layer of the nanocables. The diameter of the nanocables is determined by the reaction kinetics and relative phase diffusion. For example, when we increased the synthesis temperature to 1200 °C, the mean diameter of the nanocables increased to 80 nm.

In the above synthesis procedure, by changing the evaporation rate of ferrocene, the carrier gas flux, and the synthesis temperature, the density and size of the iron oxide nanoparticles may be adjusted. In addition, by replacing the ferrocene precursor with nickelcene, cobaltcene, or the mixture of them, the chemical composition of the magnetic particles can be changed. Through tuning dimensions, dispersion density, and composition of the magnetic particles, the magnetic behavior of the nanocables can be precisely controlled. The related detailed studies are underway.

We note that the nanocables possess a crystalline semi-conducting core and an amorphous insulating sheath layer, which make the fabrication of tiny and high efficiency field-effect transistors possible.²⁸ Most importantly, the iron oxide nanoparticles embedded in an amorphous-silica layer make the nanocables ferromagnetic, and thus new interesting electromagnetic properties and functions can be expected for the novel nanostructure.

In summary, high-purity magnetic bilayered nanocables were synthesized through a simple thermal reaction method. The nanocables are composed of crystalline SiC core grow-

ing along the $\langle 111 \rangle$ direction and amorphous silica sheath decorated with iron oxide nanoparticles. The nanocables are tens of μm in length and 40–60 nm in diameter, with a 15–20 nm thick amorphous silica sheath and an approximately 10 nm silicon carbide core. Iron oxide-containing nanoparticles in the range of 3–10 nm were dispersed evenly within the amorphous silica layer. Ferromagnetic characteristics of the nanocables have been observed up to room temperature. These novel magnetic nanocables can be promising materials for the fabrication of nanoscaled electromagnetic devices.

The authors acknowledge financial support from MEXT, Japan, and NSFC (No. 10376038), China.

- ¹Y. Zhang, K. Suenaga, C. Colliex, and S. Iijima, *Science* **281**, 973 (1998).
- ²Y. Q. Zhu, W. B. Hu, W. K. Hsu, M. Terrones, N. Grobert, T. Karali, H. Terrones, J. P. Hare, P. D. Townsend, H. W. Kroto, and D. R. M. Walton, *Adv. Mater. (Weinheim, Ger.)* **11**, 844 (1999).
- ³W. S. Shi, H. Y. Peng, L. Xu, N. Wang, Y. H. Tang, and S. T. Lee, *Adv. Mater. (Weinheim, Ger.)* **12**, 1927 (2000).
- ⁴Y. B. Li, Y. Bando, and D. Golberg, *Adv. Mater. (Weinheim, Ger.)* **16**, 93 (2004).
- ⁵Q. Li and C. R. Wang, *J. Am. Chem. Soc.* **125**, 9892 (2003).
- ⁶Z. X. Yang, Y. J. Wu, F. Zhu, and Y. F. Zhang, *Physica E (Amsterdam)* **25**, 395 (2005).
- ⁷J. C. Yu, X. L. Hu, Q. Li, and L. Z. Zhang, *Chem. Commun. (Cambridge)* **2005**, 2704 (2005).
- ⁸X. Fan, X. M. Meng, X. H. Zhang, S. K. Wu, and S. T. Lee, *Appl. Phys. Lett.* **86**, 173111 (2005).
- ⁹Y. Li, C. H. Ye, X. S. Fang, L. Yang, Y. H. Xiao, and L. D. Zhang, *Nanotechnology* **16**, 501 (2005).
- ¹⁰S. Y. Bae, H. W. Seo, H. C. Choi, D. S. Han, and J. Park, *J. Phys. Chem. B* **109**, 8496 (2005).
- ¹¹X. L. Fu, Y. J. Ma, P. G. Li, L. M. Chen, W. H. Tang, X. Wang, and L. H. Li, *Appl. Phys. Lett.* **86**, 143102 (2005).
- ¹²Y. B. Li, P. S. Dorozhkin, Y. Bando, and D. Golberg, *Adv. Mater. (Weinheim, Ger.)* **17**, 545 (2005).
- ¹³A. Chen, H. Q. Wang, and X. Y. Li, *Chem. Commun. (Cambridge)* **2005**, 1863 (2005).
- ¹⁴L. B. Luo, S. H. Yu, H. S. Qian, and T. Zhou, *J. Am. Chem. Soc.* **127**, 2822 (2005).
- ¹⁵J. H. Zhan, Y. Bando, J. Q. Hu, Y. B. Li, and D. Golberg, *Chem. Mater.* **16**, 5158 (2004).
- ¹⁶J. R. Ku, R. Vidu, R. Talroze, and P. Stroeve, *J. Am. Chem. Soc.* **126**, 15022 (2004).
- ¹⁷H. Z. Zhang, X. H. Luo, J. Xu, B. Xiang, and D. P. Yu, *J. Phys. Chem. B* **108**, 14866 (2004).
- ¹⁸Y. J. Hsu and S. Y. Lu, *Chem. Commun. (Cambridge)* **2004**, 2102 (2004).
- ¹⁹G. Z. Ran, L. P. You, L. Dai, Y. L. Liu, Y. Lv, X. S. Chen, and G. G. Qin, *Chem. Phys. Lett.* **384**, 94 (2004).
- ²⁰L. Dai, X. L. Chen, X. Zhang, T. Zhou, and B. Hu, *Appl. Phys. A: Mater. Sci. Process.* **78**, 557 (2004).
- ²¹X. C. Jiang, B. Mayers, T. Herricks, and Y. Xia, *Adv. Mater. (Weinheim, Ger.)* **15**, 1740 (2003).
- ²²X. M. Meng, J. Q. Hu, Y. Jiang, C. S. Lee, and S. T. Lee, *Appl. Phys. Lett.* **83**, 2241 (2003).
- ²³Y. C. Zhu, Y. Bando, and Y. Uemura, *Chem. Commun. (Cambridge)* **2003**, 836 (2003).
- ²⁴J. Q. Hu, Q. Li, X. M. Meng, C. S. Lee, and S. T. Lee, *Chem. Mater.* **15**, 305 (2003).
- ²⁵X. Wang, P. Gao, J. Li, C. J. Summers, Z. L. Wang, *Adv. Mater. (Weinheim, Ger.)* **14**, 1732 (2002).
- ²⁶C. X. Xu, X. W. Sun, M. B. Yu, Y. Z. Xiong, Z. L. Dong, and J. S. Chen, *Appl. Phys. Lett.* **85**, 5364 (2004).
- ²⁷T. A. Crowley, B. Daly, M. A. Morris, D. Erts, O. Kazakova, J. J. Boland, B. Wu, and J. D. Holmes, *J. Mater. Chem.* **15**, 2408 (2005).
- ²⁸The cubic $\beta\text{-SiC}$ possesses a energy gap of 2.3 eV, smaller than that of 6H $\alpha\text{-SiC}$ (3.0 eV). And doping treatment (such as nitrogen doping) can be an effective means to enhance their electrical conductivity further.